A FROZEN ISOLATION APPROACH TO BLOCKING THE WAKE-UP CALL OF LIQUIDITY SPIRALS*

Ning Zhao [a] Zhongxing Ren [a]

Jun Luo [b*]
a School of Finance, Dongbei University of Finance and Economics
b Antai College Economics Management, Shanghai Jiao Tong University

Abstract

This paper examines the role of network collaboration self-rescue from large cross-market financial institutions in the United States and Europe during financial crises, specifically in the subprime mortgage crisis and COVID-19 crisis. Utilizing small-world complex network analysis (SMW) and flight to liquidity theory, we found that the shocked system exhibits an internal instability that increases from acceleration to deceleration, during which the liquidity commonality of the network is more sensitive to provide feedback on this instability. This feedback creates a temporary strong correlation between market prices by squeezing both sides of the asset and liability through flight to liquidity. In four typical crisis simulations, we used network collaboration to block a certain range of strong correlations temporarily. By implementing a series of standards named the frozen isolation approach (FIA), we effectively reduced the liquidity commonality and stabilized the system. This study highlights the importance of timing selection, range locking, and cost control, providing insights into the difficulties of crisis rescue and improving the efficiency of network collaboration self-rescue.
Keywords: *Liquidity spiral; Isolation network; Entropy; Granger causality.*
JEL Classification: *G01; G18; H12.*

1 Introduction

1.1 Related Literature

We review the related literature about two types of problems: (i) three dimensions of stability assessment of complex systems and (ii) the network endogenous rescue strategies:

With the interaction between various financial institutions, market participants, and regulators, the financial market has formed a dynamic and complex network system. The complexity is manifested in the large number of different market participants, the interdependencies among entities within the system, and the interactions and feedback between individual entities and the overall system (Wu et al., 2024). The overall behavior of a complex system often emerges spontaneously from the interactions among individual entities and exhibits dynamic changes under the influence of external shocks a interventions. The idiosyncratic risk induced by external shocks can propagate through the complex connections among entities, leading to a 'domino effect' across the entire system (Heider et al., 2015). However, under certain conditions, external interventions can effectively mitigate systemic risk through targeted measures that block risk contagion (Jackson and Pernoud,

*Ning Zhao acknowledges the financial support from the China National Natural Science Foundation (Nos. 72001035).

2024). The essence of complex systems lies in the intricate interactions among entities, rather than merely the simple aggregation of individual behaviors (Gofman, 2017). Consequently, there has been increasing research attention on conducting holistic robustness and risk assessments of these complex systems from a macroprudential perspective (Chen et al., 2016; Gandy and Veraart, 2016; Chabot and Bertrand, 2021). In a multidimensional complex system, relying on a single indicator to evaluate the system's state is insufficient for accurately. However, the monotonic increase in information content and entropy measures as complexity grows provide a promising solution for assessing the stability of complex interrelated systems (Karaca and Moonis, 2022). Systems with higher stability demonstrate a stronger ability to maintain their internal structure and functionality in the face of external shocks or internal fluctuations, thereby reducing their level of systemic risk. Building on the work of Billio et al. (2016), we use Shannon Entropy as a measure of systemic risk from the perspective of complex systems without making any distributional assumptions about the data. Unlike traditional measures that describe the statistical characteristics of random variables, entropy measurement is based on a global description of the entire probability distribution shape, capturing higher-order information beyond the second moment, including extreme and low-probability events (Jiang et al., 2018). Additionally, by approximating the distance to a uniform distribution, entropy measurement can reflect structural changes in the overall risk distribution of the system (Ebrahimi et al., 1999). In this paper, we propose using entropy as a measure of systemic risk. We also consider CoVaR and MES, two classical methods that characterize systemic risk through tail returns, to corroborate the robustness of entropy measurements. CoVaR is considered a milestone contribution in systemic risk research; Adrian and Brunnermeier (2016) use the conditional quantile method to measure the risk contribution of institutions and the macro market by assessing tail dependency. Building on this, MES measures the marginal expected shortfall of institutions at the left-tail quantile level of the system (Acharya et al., 2017).

With the innovation of derivative financial instruments and the increasing interconnectedness of financial institutions, accurately characterizing the complexity and dynamic nature of financial systems is crucial for better identifying potential risks and implementing targeted prevention and control measures. In the real world, factors such as asset-liabilities relationships (Gandy and Veraart, 2016), asset prices co-movement (Billio et al., 2012), and similar risk exposures (Ahnert and Bertsch, 2022). all contribute to the complexity of the system. The complex connection relationship is often assessed using a network model, in which nodes represent the institutions and weighted edges represent different types of connection(Gandy and Veraart, 2016). Network edges formed by different channels can contagiously spread idiosyncratic risk from a single node outward to the entire network (Billio et al., 2012). Acemoglu et al. (2015) argue that after the 2008 financial crisis, the findings of research based on risk contagion from a network perspective drove the implementation of many policies. The idiosyncratic risk of a single node does not react directly at the level of the market as a whole, but gradually accumulates through contagion

within the network(Elliott et al., 2014). Thus the modeling of network connections can describe the risk contagion that has occurred within a certain range, especially the extreme risk measure in the crisis interval and the portrayal of network nodes in a multidimensional perspective enhance the prospectivity and accuracy of risk early warning (Wang et al., 2017, 2021). Paltalidis et al. (2015) find that the sovereign credit risk channel dominates amplified systemic risk in the European interbank network and that risk propagation losses are positively correlated with size and connected degree. Jackson and Pernoud (2024) demonstrate through numerical simulations in inter-bank asset-liabilities network with a "center-periphery" structure, the credit default bankruptcy of the core bank has the most significant impact on system stability. However the specialization of financial data can only focus on a single type of risk (Cincinelli et al., 2022), plus its inherently unavoidable lag are unsuitable for a real-time description of systemic risk (Wang et al., 2018). Market data networks, on the other hand, are able to overcome these shortcomings, with the impact of external shocks, fundamental fluctuations, and financial developments feeding back through stock prices in an integrated way and affecting the overall state and correlation structure of the market in real time (Antzoulatos et al., 2016). The direction of interaction between nodes and the level of risk contribution can be reflected through directed edges and connection degree in the market network (Pacelli et al., 2022). Billio et al. (2012) takes principal-components analysis and Granger-causality networks, and apply them to the monthly returns of hedge funds, banks, broker/dealers, and insurance companies. He finds that the correlation during the 2008 financial shock was significantly stronger than that during the stable period. They also show that the highly correlated network increased the risk level of the system. Through a network based model of the over-the-counter interbank lending market, Gofman (2017) finds that larger institutions with higher connections take liquidity as a carrier of risk contagion during shocks, which impacts the stability of the financial system. Using the data of 90 banks in 28 countries from 2003 to 2018, Hué et al. (2019) use the Granger connectedness casually network to evaluate the interconnectivity between banks and note that banks with higher connectedness contributed more systemic risk during the shocks than banks with lower connectedness. Stock returns can serve as a comprehensive feedback on the state of the company and reflect the lasted market information(Wang et al. 2018). Dynamic network studies on stock trading data mainly focused on asset price co-movement(Cincinelli et al. 2022) and risk spillover(Grillini et al. 2022). The studies on spillovers focuses on tail risk correlations between institutions, capturing risk spillover behavior under extreme conditions through the unexplained portion of each other's returns(Pacelli et al. 2022). In contrast, research on co-movement focuses on the part of stock returns that explains each other, and complex networks constructed based on linear Granger causality tests measure the most direct causality in the co-movement of stock returns between institutions(Balboa et al. 2015). Based on the results of the Granger causality test, directed networks can be constructed and used to reflect the asymmetry of the interactions between nodes(Hong et al. 2023); meanwhile, the structure changes can reflect the risk linkages between the nodes and the whole system (Caporin and Cos-

tola 2022). Utilizing the network approach to capture the dynamic states of the complex system, (Nivorozhkin and Chondrogiannis 2022)show that the density of the connected network shows a positive correlation with the level of systemic risk; (Geraci and Gnabo 2018) also argue that networks with a higher degree of centralized connected nodes has a higher level of risk contagion.

Overiew the process of systemic risk formation, the study suggests that the core behind the risk contagion and accumulation are the deterioration of liquidity and coherent behaviours(Elliott et al. 2014). With the deleveraging of financial institutions, the role of market liquidity effects in financial networks has overtaken the credit risk exposure of debt intermediation as the main trigger for large-scale risk contagion(Chen et al. 2016). When facing an external shock, the market receives a wake-up call, the institutions start similar fire sale behaviour gradually because of the rising default risk, margin demand and liquidity hoarding expectations (Ahnert and Bertsch 2022). Viral Acharya and Pedersen (2005a) claims market downturns and liquidity "dry up" significantly affect the risk premium of securities. The more institutions that engage in this behaviour, the faster the asset prices in the market deteriorate, and the decline in market prices prompts more institutions to hoard liquidity until the market liquidity appears to be exhausted, exhibiting a spiral of deteriorating market liquidity and funding liquidity. Therefore, another important contribution of this paper is to propose a liquidity commonality mitrics of market and institutional co-movement as a measure of the level of risk contagion within the system in a network perspective. The coherent behavior of institutions leads to a further deteriorated liquidity spiral and a surge in correlations(Niţoi and Pochea 2019). Similar fire sale behaviour prompts the scale effect of the liquidity spiral and leads to a high correlation between institutions, which indicates high liquidity commonality(Choi and Cook 2012). Brunetti et al. (2019) find interbank market liquidity was impaired by hoarding behaviour during the 2008 global financial crisis and also finds that the risk contagion increased during this period. Researchers have also shown that liquidity commonality is sensitive to market environments characterized by shocks, such as more volatile and large risk contagion. Rösch and Kaserer (2014) find that the liquidity commonality of the four major German stock indices was higher during the 2008 shocks. The liquidity commonality can be enhanced, and the system experiences a liquidity depletion spiral at the same time. More relative research is available from Chordia et al. (2001), Markus K. Brunnermeier and Pedersen (2008b), Kamara et al. (2008), Kempf and Mayston (2008), Hameed et al. (2010), NÆS et al. (2011), Karolyi et al. (2012) and Moshirian et al. (2017).

Based on the risk contagion process, some researchers have begun to explore the means of blocking and systematically rescue. By evaluating a variety of central bank monetary policy instrument, Sedunov (2021) finds that liquidity injections can bring a decline in the level of U.S. interbank risk contagion and a positive feedback in market conditions during a crisis. In the 2008 global financial crisis, the Federal Reserve's liquidity injections provided financial institutions with substantial asset guarantees and an expanded discount window, which allowed key financial institutions to remain solvent and avoided a sys-

temic financial meltdown(Bolton et al. 2009b). However, while providing short-term relief from liquidity risk, frequent liquidity injections can also lead to the market inefficiencies and undue profit-taking by some institutions(Viral. Acharya et al. 2011). The target of the central bank's liquidity injection is often the larger institution with a higher market share, and the larger institutions will firstly satisfy their own liquidity holding demends after obtaining liquidity support, thus resulting in some of the smaller institutions in the market not being able to get the necessary liquidity supplementation and being given up, leading to an incomplete and effective liquidity injection(Bolton et al. 2009b, L. A. Bebchuk and Goldstein 2011b).Gofman (2017) propose that, the expectations of rescue can cause some large institutions to neglect their own risk management and exacerbate maturity mismatches on their balance sheets, creating a moral hazard problem. Freixas (2009)argue that as a crisis develops and liquidity diminishes, authorities need to inject much more liquidity at lower interest rates than predicted by the standard monetary policy mode. "Much more liquidity" has also become a factor in the abnormal increase in inflation. Considering the disadvantages of liquidity injection, some researchers presented by (Viral Acharya and Yorulmazer 2008, Viral Acharya et al. 2012) begin to pay more attention to the 'pre-crisis' interventions, they try to strat within the network to achieve an self-rescue effect without additional liquidity injections by blocking risk contagion. Rogers and Veraart (2012) propose an internal rescue model in which liquidity is mobilized and reallocated from within the network to prove the effectiveness of internal rescue among banks. They figure out that the cost of consumption of an internal rescue among banks is less than the loss from the risk spillover of a bank's failure to other banks in the network. Wu et al. (2024) suggests that the overall level of robustness of the network can be improved by the internal control method of removing edges and nodes from the network. The core of removing edges and nodes is to utilize the collaboration of nodes within the network for resource reallocation to better respond to changes in the external environment(Holland 1992). But, the systematic rescue within the network requires certain conditions. Bernard et al. (2022)note that the self-rescue plan requires regulators to participate, at least assisting in the operation of rescue. During the subprime mortgage, the German government once appealed to the institutions in the system to alleviate the short-term effects of the shock through creditor write-downs ; however, no specific implementation process for stimulating institutional participation was designed, so no surprise results occurred. In addition, although researchers have proposed theoretical models for systematic collaborative rescue, they have not determined the specific intervention targets, timing, and ways to participate in collaborative rescue in empirical studies, and how to maximize the effect while minimizing the cost is still an urgent issue(Viral Acharya et al. 2012). A more specific and generalized set of studies is needed.

2 The wake-up call in network

3 Methodology

The effectiveness of FIA-based network collaborative rescue is ensured through two phases. In the first phases, We demonstrate the effectiveness of the FIA from the perspective of three dimensions: overall systemic risk, network structure, and liquidity commonality. (i) By estimating the growth rate of Shannon Entropy, FIA explores the process of risk increasing and decreasing before the systemic risk fully outbreak. We investigate the possible interval of "pre-active" interventions by analysing the rate and total amount of risk accumulation. (ii) The FIA uses market data to simplify the system into a Granger causal network composed by nodes (institution) and connected edges (causal relationships) to capture the earliest direct correlations in the 'wake-up' process. At the same time, we use network density to further demonstrate the process of increasing connectivity and scale during the crisis, in order to infer the effectiveness of the removing nodes strategy. (iii) The FIA estimates the network liquidity commonality, and by confirming the role of liquidity commonality in the 'wake-up' as a driver of systemic outbreaks, we argue that liquidity commonality can be used as a basis for determining the validity of the FIA's simulations.

In the second phase, by comparing the simulated remove strategy in accordance with different time and constraint optimize method, the article argues the existence of a cost effective optimal solution for FIA. Compared to samply remove nodes by the connection degree, we find that the optimisation model developed based on 3.3 is able to achieve the minimum cost while ensuring the validity of the determination.

3.1 Systemic risk measurement and crisis decomposition

With a myriad of interacting elements and diverse participants, the financial market forms a dynamic complex system. In this paper, we utilise Shannon Entropy as a measure of system uncertainty from an information theoretical perspective. Let x be defined as the random variables in the probability space(Ω, F, P), we consider a probability experiment with n uncertain outcomes, and let the outcomes $x_1, x_2, \cdot, x_n$ each with discrete probabilities $p_i (i = 1, 2, \cdot, n)$, the entropy of a probability measure p is defined as:

$$H_n(p) = \sum_{i=1}^{n} p_i \ln p_i \tag{1}$$

$$H(x_{jt}) = -\sum_{j=1}^{m} C \cdot x_{jt} \log x_{jt} \tag{2}$$

lnp_i is stated as the amount of information required to convey the shortest length of information, H denotes the weight expectation of the function lnp_i. That is, the weighted average of the shortest amount of unknown information is explored each time, and it is also the expected statistics of the frequency of events, as $0ln0 = 0$, the function H is called

entropy in information theory. The entropy of a continuous random variable X whose density function is $p(x)$, then the entropy is defined as:

$$H(x) = -\int_{\Omega} p(x) \, lnp(x) \, dx \tag{3}$$

Based on the monotonic relationship with the system uncertainty, Shannon Entropy can effectively reflect the risk status of complex interconnected systems.We also employ $\Delta CoVaR$ and MES as metrics of systematic risk to corroborate the robustness of the entropy[1].

$$v = \frac{(E_t - E_{t-1})}{t} \tag{4}$$

Furthurly, we decompose the risk formation process under successive shocks. Referring to Eq 4, we calculate the entropy growth rate v as a measure of system stability changes. We find that the stability of the system in different shock events will show a similar process of initial entropy increase and then entropy decrease, which is manifested as the surge and dissipation of strong correlation within the system.

3.2 Network definition and liquidity spiral measurement

We use the granger casuality network to capture the direct linkage relationship. The network consist with nodes and edges: n nodes of financial institutions, and the edges obtained by the granger causality test. The correlation Granger causality test, introduced by Granger (1980), can capture only the leading lag relationship constructed by the correlations of financial institutions. The directed frontiers from Granger causality quantify the risk contributions or impacts of financial institutions during shocks (Wang et al. 2017, Wang et al. 2021). We adopt the Granger causality matrix to explore the changes in correlations within the liquidity spiral interval. the increasing number of institutions increases the strong correlation, which strengthens co-movement in the system. This scale effect triggers the liquidity spiral, which increases the liquidity commonality and dries up liquidity in the system. We perform a pair-wise Granger causality test to determine the directed edges between the correspond institutions i and j.

$$\beta_{ij} = \begin{cases} 1if \ i \ Granger \ cause \ j, \\ 0else \end{cases} \tag{5}$$

We conduct Granger causality on the return series of institutions i and j. If i has Granger causality on j (its p value is less than 0.05), element $\beta_{i,j}$ takes a value of one, with $\beta_{i,j} = 1$ if node i Granger-causes node j and $\beta_{i,j} = 0$ otherwise. Thus, we can obtain the adjacency matrix B consist of 0 and 1 in Eq (2) to represent the degree of the connection between financial institutions. Meanwhile, since the adjacency matrix represents the direction of the edges in the network, we set the elements on the main diagonals$\beta_{ij} = 0, (i = j)$.

[1]The calculation of Delta CoVaR and MES are shown in Appendix A

$$B = \begin{bmatrix} \beta_{11} & \cdots & \beta_{1n} \\ \vdots & \ldots & \vdots \\ \beta_{n1} & \cdots & \beta_{nn} \end{bmatrix} \tag{6}$$

In the fincncial network, the impact of liquidity factors on asset price is considered to be the most sensitive to external shocks(Viral Acharya and Pedersen 2005a). Fire sale and chain default bankruptcies induced by liquidity risk will lead to changes to the network structure, and the liquidity commonality brought by widespread liquidity risk will lead to a spiral of risks at the market level and the institutional level, and even to the outbreak of systemic risk. Network models provide us with a useful bridge to establish links between the macro market and institutions, based on which we use a regression model to capture the degree of liquidity commonality between market liquidity and funding liquidity.The liquidity commonality is denoted as R^2 in the regression model to describe the market liquidity and institutional liquidity. A higher (lower) R^2 value could indicate a higher (lower) liquidity co-movement level across markets and institutions. We then measure the liquidity commonality between the markets and institutions based on the trend of R^2 to identify whether the responses of markets and institutions cause increased spirals during the shocks. Specifically speaking, the left hand of the model is market liquidity, which can be considered as the expression of a certain volume of institutional liquidity in the market (Brockman et al. (2009), Chordia et al. (2001), Lesmond (2005)). Its measurement can be classified by depth and width. The width is reflected by the extent to which the current trading price deviates from the middle market price (i.e., bid-ask spread). The depth is reflected by the maximum volume of transactions with stable prices (i.e., Volume). As noted by Markus K. Brunnermeier and Pedersen (2008b) lower volumes and wider spreads lead to higher liquidity premiums and losses on existing positions. Brockman et al. (2009) Using spread and depth data from forty-seven stock exchanges, which find that the commonality between firm-level liquidity (i.e., institutional liquidity) and exchange-level liquidity (i.e., market liquidity) has a cross-industry spillover effect. Rösch and Kaserer (2013) investigate liquidity behavior by bid-ask spread and volume, observing large jumps in liquidity commonality during shocks. Here, we adopt WS_t as market liquidity and P_{mid} as the market middle price (Hameed et al. (2010)):

$$WS_t = \frac{\frac{1}{n_t}\left(\sum_{i=1}^{N} a_{i,t} \cdot n_{i,t} - \sum_{i=1}^{N} b_{i,t} \cdot n_{i,t}\right)}{2Pmid_{i,t}} \tag{7}$$

where $a_{i,t}$ and $b_{i,t}$ are the highest and lowest stock prices of institution i at time t, $Pmid_{i,t}$ is the mid-price from $a_{i,t}$ to $b_{i,t}$, $n_{i,t}$ and n_t represent the volume of individual institution i and market at time t, and N is the total number of institutions.

The measure of institutional liquidity on commonality includes multiple factors of the institution, which we describe below. The most common direct liquidity influences at the institution level include the daily transaction volume VO, closing price P, daily market value MV and annualized 5-day standard deviation of daily log-return σ_r, which can re-

flect the time-varying features of market-wide liquidity and trading activity commonality (Chordia et al. 2001). We let $\sigma_{r,t} = std(r_t, \cdot, r_{t+4}) \times \sqrt{n}$ denote the standard deviation of daily log-returns (i.e., r_t, r_{t+1}, ..., r_{t+4}) calculated in n=252 day increments. We measure institutional liquidity with the four factors mentioned above, measure market liquidity with WS after logarithmization in Eq 7, and build a regression model such as Eq 8

$$logWS = a_0 + a_1 logVO + a_2 logP + a_3 logMV + a_4 \sigma_r + e \tag{8}$$

In the remainder of the paper, our models include the dependent variable $logWS$ and all the standard control variables in Eq 8. To examine the impacts of financial shocks on liquidity commonality and therefore scrutinize the individual data in panel-data regression analysis, or our regression analysis, we use a log-log specification.

we design the Frozen Isolation Approach (FIA) to address the sharp increase in correlations during the liquidity spiral. In the FIA, our study utilizes a removal strategy to block the risk propagation by removing institutions (nodes) and linkages (edges) within the network in order to isolate the spread of liquidity spirals. FIA does not allow any institution to gain additional liquidity, as this liquidity leads to moral hazard and other issues. FIA is intended to stop boiling by reducing the heat at the bottom of the pot (i.e., the system) rather than by pouring in cold water (i.e., excess liquidity).

We combine Granger causality with a grey correlation series assignment approach to simulate a market in which a few institutions are isolated from the whole system. When institution i is isolated from the market, we consider it to be removed from the connected edges of other institutions in the network. The values of the corresponding rows and columns are set to zero in the matrix, i.e., $\beta_i = 0$. And then get the adjacency matrix $B^{'}$ after removing n institutions. We use the adjacency matrix before and after isolation as a weight matrix representing the co-movement relationship between institutions. Let X be the vector of independent variables representing institutional funding liquidity. We define the simulated independent variable as: $X_{T\times N} = X_{T\times N} B_{N\times N}$; $X^{'}_{T\times N} = X^{'}_{T\times N} B^{'}_{N}$. And by the regression model in Eq 8 we calculate the liquidity spiral in the network as the average R^2 of the regression result. After implementing FIA by the highest degree node removing strategy, we update the weight matrix $B^{'}$ at the same time. Corresponding to the adjacency matrix $B^{'}$ after removing n nodes, we can calculate the average intra-network correlation of $N - n$ institutions after external intervene as the liquidity spiral degree in the market under the FIA simulation results denote as R^2_{sim}. R^2 is denoted as the reference series x_0 and R^2_{sim} is the calculating series x_i, which are used to calculate the Grey relation degree time series $\gamma(x_0(t), x_i(t))$ in Eq 9:

$$\gamma\left(x_0\left(t\right), x_i\left(t\right)\right) = \frac{\underset{i}{min}\underset{t}{min}\left|x_0\left(t\right) - x_i\left(t\right)\right| + \varepsilon \underset{i}{max}\underset{t}{max}\left|x_0\left(t\right) - x_i\left(t\right)\right|}{\left|x_0\left(t\right) - x_i\left(t\right)\right| + \varepsilon \underset{i}{max}\underset{t}{max}\left|x_0\left(t\right) - x_i\left(t\right)\right|} \tag{9}$$

We use a grey correlation algorithm to compare the average degree of correlation in the network after implementing the FIA as a percentage of the original marketcalculating grey correlation coefficients provides us with a dynamic correlation method for comparing the

effect of conducting FIA at different times and quantity of nodes. The series is multiplied by the R^2_{sim} of Eq 8 as a coefficient to represent the degree of liquidity spiral after the FIA, referring to (Chordia et al., 2001; Hameed et al., 2010; Karolyi et al., 2012; Moshirian et al., 2017) Rösch and Kaserer, 2014. We calculated the percent change of liquidity spiral caused by FIA in a given time interval T.

$$Percent\ Change = \frac{\sum_{t=1}^{T} R_t^2 - \sum_{t=1}^{T} R_{sim,t}^2}{\sum_{t=1}^{T} R_t^2} \tag{10}$$

The isolation design in the FIA is based on the fact that the individual financial instruments suspend trading and announce redemption during bad institutional situations. If this thinking is expanded, the transactions of some institutions can be suspended in the short term. Co-movement formed in shocks causes enormous, highly correlated institutions to contribute more systemic risk and become the main contributors to the spillover risk (Billio et al., 2012; Hué et al., 2019). Former Fed chair-man Paul Volcker suggests that regulators manage the risk of interconnected firms by "curtailing their interconnections, or limiting their activities" (Volcker 2012). The FIA simulates the situation in which regulators limit the activities of identified institutions by suspending trading (named isolation).

3.3 Optimization model for FIA

Based on the institutional correlation network and liquidity spiral formation process. We furtherly propose the optimal conditions for the implementation of FIA. In the network, connectedness between institutions become channels for the co-movement behaviours, and FIA 'melts down' trading for a small number of institutions from the network by removing nodes, thereby blocking risk contagion and achieving endogenous rescue within the network. under the framework of network and liquidity spiral, we transform the endogenous rescue problem of financial institutions into an optimal control problem for nodes within a complex network. The core of the FIA is to remove edges between kernel nodes and another marginal node in the network, releasing the correlation aggregation in the pre-crisis period, thus weakening the coherent behaviour of institutions during the crisis and impeding further contagion of liquidity risk. Therefore, based on the analysis of risk process in 3.1, choosing the right time of implementation as well as the isolated target object node is the key to the effective implementation of FIA. On this basis the simulation of removing nodes at different points in time is conducted to compare the effect of FIA's policy implementation.

After defining the optimal timing to implement FIA, a more complex task is the target nodes of FIA. The topological characteristics of a network have significant influence on the ability to transmit risk within it(Ding et al. 2017). Thus we need to achieve controllability of the entire network by removing some of the nodes from the system. Kitsak et al. (2010) claim that there is a distinct small-world character in financial networks, where a few nodes are significantly more connected than others in the network. Unlike stochastic networks, this "centre-periphery" network structure leads to the degree distribution fat-

tailed, a few centralized nodes exhibit stronger correlation aggregation and risk spillover effects.It will amplify the propagation and spread of risk during a crisis. The choice of the minimum number of nodes in global control depends on the degree distribution of nodes in the network, removing centralised nodes rapidly increases the network diameter and affects network stability(Albert et al. 2000), thus We use the degree distribution as a measure of the overall stability of the network and adopt a maximum degree strategy to select nodes and gradually remove them from the network. As the number of removed nodes increases, the degree of correlation in the network decreases, but the two do not show a simple linear relationship. In addition to this, simply increasing the number of removed nodes does not take into account the cost of control. A higher number of institutions entering the FIA implies a monotonically increasing control cost, so we need to trade-off between minimising the cost and the most efficient isolation effect. In this regard, We use a randomly generated uniform distribution as the a posteriori distribution and use the cross-entropy loss function to measure the KL distance between the node degree distribution and the uniform distribution in the network as an evaluation metric. Thus, we design a constrained optimisation model with the penalty cost function to solve for the minimum number of nodes to be removed to make the whole network optimal. A smaller KL distance indicates that the current network is closer to a relatively stable status.

In the directed graph, n is the number of nodes remaining in the network after FIA, x_i denotes node i in the network, The random variable $d(x)$ is an indicator of the degree of nodes in the network defined as follows:

$$d\left(x_k\right) = \sum_{j=1}^{n} \beta_{i=k,j} + \sum_{i=1}^{n} \beta_{i,j=k} \tag{11}$$

$d(x_k)$ denotes the total degree of connection of node k in the network, let $p(x)$ be the PDF of the node degree distribution in the network, and $q(x)$ is a uniform distribution representing a fully connected network with the same number of nodes. Referencing Breuer and Csiszár (2013), we use cross-entropy function to measure the distance between two distributions:

$$L\left(n\right) = D_{KL}\left(p|q\right) = \sum_{i=1}^{n} p\left(x_i\right) \log\left(\frac{p\left(x_i\right)}{q\left(x_i\right)}\right) \tag{12}$$

$L(n)$ is a function of the remaining nodes n in the network, and we abbreviate the KL distance between the two distributions after removing the nodes as $D(x)$. And in order to take into account the cost minimisation objective, we use the cumulative market capitalisation of the removed institutions as a percentage of the total market capitalisation as a penalty function for the cross-entropy function:

$$C\left(n\right) = \sum_{i=1}^{n} c\left(x_i\right) \tag{13}$$

where $c(x_i)$ is the market capitalisation of institution i as a percentage of total market

value, we use market capitalisation as a proxy variable for the cost of internal rescue. $C(n)$ is a monotonically increasing penalty function representing the total value of the cumulative costs required under the condition of isolating n institutions. Our goal is to minimise the cross-entropy loss function, since both $L(n)$ and $C(n)$ take values between (0,1), we construct our constrained optimisation model by summing the two using a simple linear relationship:

$$f(n) = F(L(n) + C(n)) \tag{14}$$

$F(\cdot)$ is a fitted function with quadratic term, which is used to fit the numerical calculation results of $L(n) + C(n)$ into a continuous convex function form. Because $C(n)$ is monotonically increasing in the definition domain, and KL divergence $L(n)$ is a convex function, the linear combination of the two also meets the convexity requirement. For the function $f(n)$ of the random variable n, we minimize the objective function within the defined domain to obtain the optimal control number of FIA:

$$\begin{aligned} &arg \min_{n} f(n) \\ &s.t. n \in (1, N) \end{aligned} \tag{15}$$

$f(n)$ represents the global constrained optimization model with penalty function, and we solve the optimal isolation number n in a certain scenario by minimizing the objective function. We adopt our model to solve the optimal number of institutions in FIA for four shock events. Through removing a certain number of nodes from the network, we compare the declining effect of liquidity spiral with original market. And at the same time comparing the suppression effects between traditional liquidity injections and endogenous rescue strategies under the complex network perspective.

4 Empirical Work

In this section, we apply our market dataset from US and EU institutional data to assess the validity of FIA. In the first part, we measure the systemic risk, dynamic network destiny and the degree of liquidity spiral in three dimensions within the market and classify four shock intervals. In the second part, we discuss the optimal time and number of institutions in FIA for each shock separately. Meanwhile, we examine the contrast between the two regulatory ideas of 'too big to fail' or 'too connected to fail'. By this way, we try to answer the question about when and how to block the wake-up call.

4.1 An introduction of dataset

Research on the financial crisis relies on two main types of data sources, balance sheet data and market data, which have been studied in various existing works, e.g., (Choi and Cook, 2012; Sedunov, 2021; Zedda and Cannas, 2020) using the former dataset and (Buse et al.,

2022; Ma et al., 2022; NicolaBorri and diGiorgio, 2021; Niţoi and Pochea, 2019) using the latter one. Notably, detailed balance sheet data can more accurately reflect the risk at the institutional level, as this information is typically updated on a quarterly basis. When exploring the rapid spread of risks under financial shocks and recovery of risks in the system, quarterly data are not sufficient for describing the time-varying changes in the underlying risks. Moreover, the immediate adjustments of financial institutions after the shock may conceal the traces of risks, which is detrimental to the analysis of the risk structure characteristics (Adrian and Brunnermeier, 2016). Differing from the balance sheet data, the market data mainly concern stock prices and credit default swap (CDS) premium spread, which could also be used to reflect the risk exposure in financial institutions due to financial shocks. For the sake of data calculation, in this paper we use stock prices and select all U.S. and E.U. financial institutions that issue both stocks and CDS as the sample, thus including a total of 93 U.S. institutions and 81 E.U. institutions. U.S. data are provided by DataStream[2], and the E.U. data are provided by Bloomberg[3] and the Capital database[4].

In our research, we focus on the period from January 3, 2006, to April 12, 2022, which encompasses the main shock events over nearly two decades. Our data include a sample of seven financial institutions' factors, including opening and closing prices, high and low prices, daily transaction volume, average bid ask spread, and mid-price.

4.2 Risk interval and liquidity spiral in the network

We identify shock events as well as systemic stability in three dimensions: systemic risk, network density, and liquidity risk. In Figure 1-A, we use Shannon Entropy, Dleta CoVaR and MES as an overall metrics of systemic risk. We find that the three show very similar trend on the risk measurement. More details about the calculation and results of Delta CoVaR, MES are shown in the appendix. In Figure 1-B, we use network destiny to capture the co-movement within institutions. It's obvious that during the market downturn, Transient strong correlations will form between institutions, causing a surge of correlations within the network. The sharply rise up of network destiny during the shock intervals will strength the fundamental deterioration and risk contagion. This strong correlation enhances the homogeneity between institutions within the network. Similar to systemic risk indicators, network density shows a sharp increase in times of financial turbulence. At the same time, network density changes more rapidly than systemic risk, and then declines back to its normal level as the shock event ends. In Figure 1-C, we calculate the liquidity spiral within the network, and also collect the shock events and liquidity injections during the sample period. The black curve presents the liquidity commodity, which is used to measure the co-movement between market liquidity and institutional funding liquidity, the higher level of liquidity spiral indicates the greater the likelihood of downward liquidity conditions in the system and the higher the liquidity risk. The red dashed

[2]DataStream dataset is from EIKON integrated terminal, https://eikon.refinitiv.com/
[3]From https://www.bloomberg.com/
[4]From https://www.capitaliq.com/

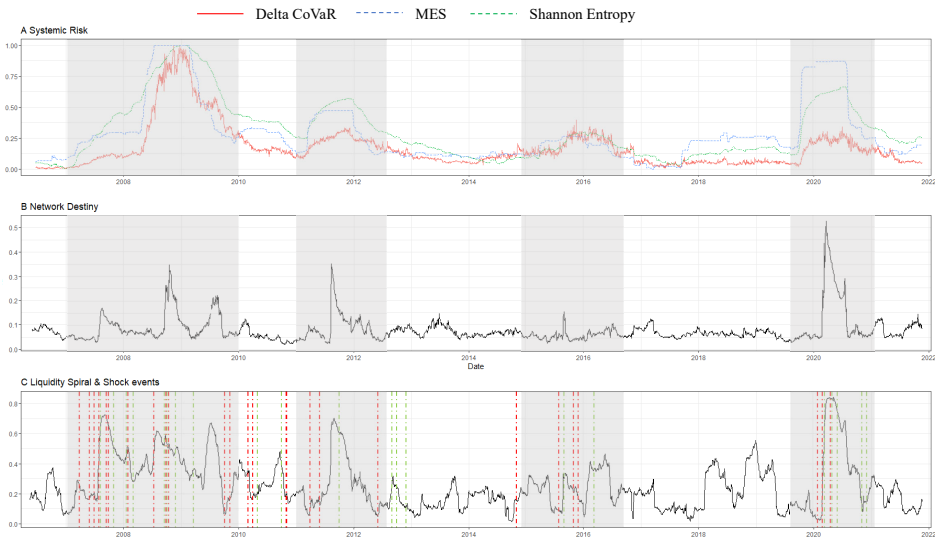

Figure 1: Three dimensional risk measurement and risk interval

lines represent the shock events, and the green dashed lines represent the liquidity injections or rescue policies implemented by the Federal Reserve and government in response to the crisis. It can be seen that liquidity risk is more sensitive to the external environment changes than systemic risk and network structure indicators. The shock events promotes the liquidity spiral rise up and the liquidity injection and release this temporary strong correlation. Based on the results of the three dimensional risk measurements, we divide four crisis intervals in the shade areas over the sample period: The first shaded area marks the subprime mortgage crisis period occurring in approximately 2008 (2008 shock from July 2006 to August 2009); the second one marks the period of the European debt crisis occurring in approximately 2010 (2010 shock from August 2009 to December 2012); and the third one and fourth one mark the stock market shock period in 2015 (2015 shock from July 2014 to August 2017) and the COVID-19 event in 2020 (2020 shock from September 2019 to the end of the sample) respectively.

4.3 Optimal timing of FIA

We accurately identify four increased intervals of systematic risk for four shocks as captured by Shannon Entropy and the growth rate. We use the shaded area to mark the corresponding intervals of changes in systematic risks according to the different four shocks. In order to further study the risk aggregation process in each shock event, take the measure of Shannon Entropy, we further calculate the growth rate of Entropy as an evaluation metrics. In each of the shocks shown in the shaded area, we decompose the crisis process and use it to identify two phases and three points in time. we divide the process of increasing risk due to shocks into the risk accumulation stage (from start points to the maximum growth points), the risk surge stage (from maximum growth points to highest risk value point). we denote the start and end points of the crisis as SP and EP respectively, the maximum growth rate points are defined as the risk aggregating points (RAP), and the highest risk

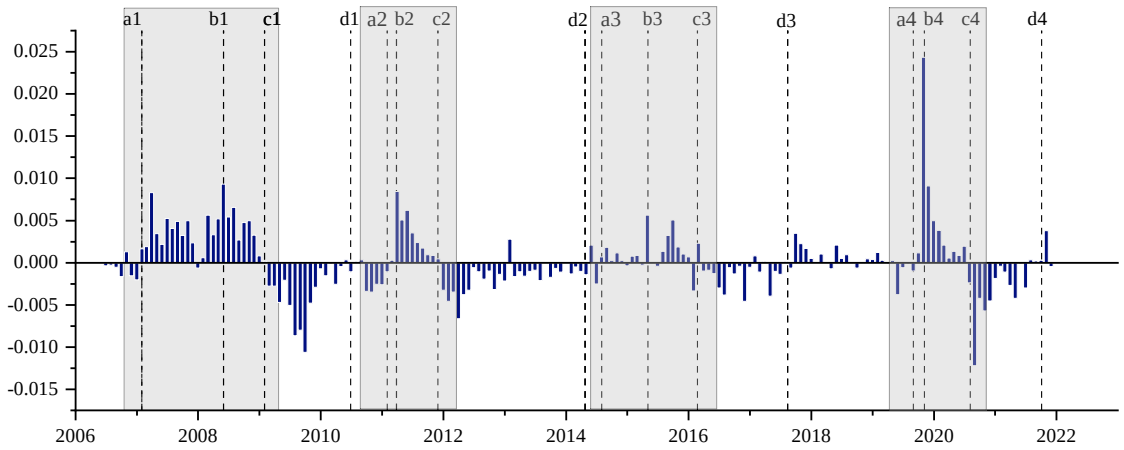

Figure 2: Growth rate of Shannon Entropy

value point in the shade areas of figure3 was defined as the maximum risk points (MRP). As shown in figure 2, we mark the corresponding four points during single shock as a_i, b_i, c_i and d_i, where $i = 1, 2, 3, 4$ is the index of shock events.

The risk growth speed in each shock is similar, so the magnitude of the highest risk value point is determined by the duration. In Table 1, the average difference between the average growth rate of the four shocks is only 0.002: 0.005 for the 2020 shock, 0.003 for the 2008 and 2010 shocks, and only 0.001 for the 2015 shock. The variance is 0.0001 for all three shocks except for the 2020 shock, in which the variance is 0.0099. In Table 1, Start means the indicator begins to increase, peak indicates it has reached the peak value and end means that the risk indicator no longer decreases. Similarly, the Growth Rate start indicates the start point of the continuous positive entropy growth rate, the peak indicates the maximum growth rate of increase, and the end indicates that the growth rate becomes negative after this point. Mean and variance denote the mean and variance of the growth rate in the shock interval.

The shock with the longer range of risk surge yields a higher risk peak. The stage of risk accumulation (Stage $a_i - b_i$) indicates the interval in which the risk appears to be rising at a positive rate and continues to increase to the maximum speed. The stage of risk surge (Stage $b_i - c_i$) represents the interval in which the risk begins to decline from the maximum growth rate until reaching the highest risk value. Thus, the dotted line marked as $a_i (i = 1, 2, 3, 4)$indicates a positive starting point for risk, bi denotes the maximum rate of increase and c_i denotes the highest risk point after which the growth rate begins to turn negative: $v \leq 0$. The highest risk peak occurs at the 2008 shock. The 2008 shock exhibits the longest accumulation stage a1-b1 and surge stage b1-c1, which last 17 and 6 months, respectively. The risk peak at the 2010 shock is similar to that of the 2020 shock. The accumulation stage for the 2010 ($a_2 - b_2$) and 2020 ($a_4 - b_4$) shocks are both shorter than a1-b1, while the length of the surge stage is similar for all three. Both the 2010 shock ($a_2 - b_2 - c_2$) and 2020 shock ($a_4 - b_4 - c_4$) have shorter accumulation stages and longer

Table 1: The risk turning point in 4 shocks in US

Time	Event	Start	Peak	End
2008 Entropy	Date	7-Jan	9-Jan	11-Jan
	Entropy	-3.0837	-1.0944	-2.5848
2008 Growth Rate	Date	7-Jan	8-May	9-Jan
	Speed	0.0017	0.0093	0.0001
	Mean	0.0038		
	Std	0.0024		
2010 Entropy	Date	11-Feb	11-Nov	14-Jun
	Entropy	-2.6017	-1.961	-2.9684
2010 Growth Rate	Date	11-Feb	11-Mar	11-Nov
	Speed	0.0003	0.0084	0.0005
	Mean	0.0030		
	Std	0.0028		
2015 Entropy	Date	14-Jul	16-Feb	17-Aug
	Entropy	-3.0049	-2.5201	-3.0274
2015 Growth Rate	Date	14-Jul	15-Apr	16-Feb
	Speed	0.0007	0.0056	0.0023
	Mean	0.0011		
	Std	0.0020		
2020 Entropy	Date	19-Sep	20-Jun	21-Nov
	Entropy	-2.8577	-1.7938	-2.5842
2020 Growth Rate	Date	19-Sep	19-Oct	20-Jun
	Speed	0.0012	0.0243	0.0019
	Mean	0.0050		
	Std	0.0073		

Notes: Table 1 shows the event time and systemic risk level of four shocks in the US market. The row Entropy corresponds to three columns: start, top, and end, which are used to describe the beginning, maximum, and end of systemic risk in a shock respectively. The growth rate at the top point means the maximum growth rate, while the growth rate at the end point is 0 corresponding to the maximum systemic risk at this time.

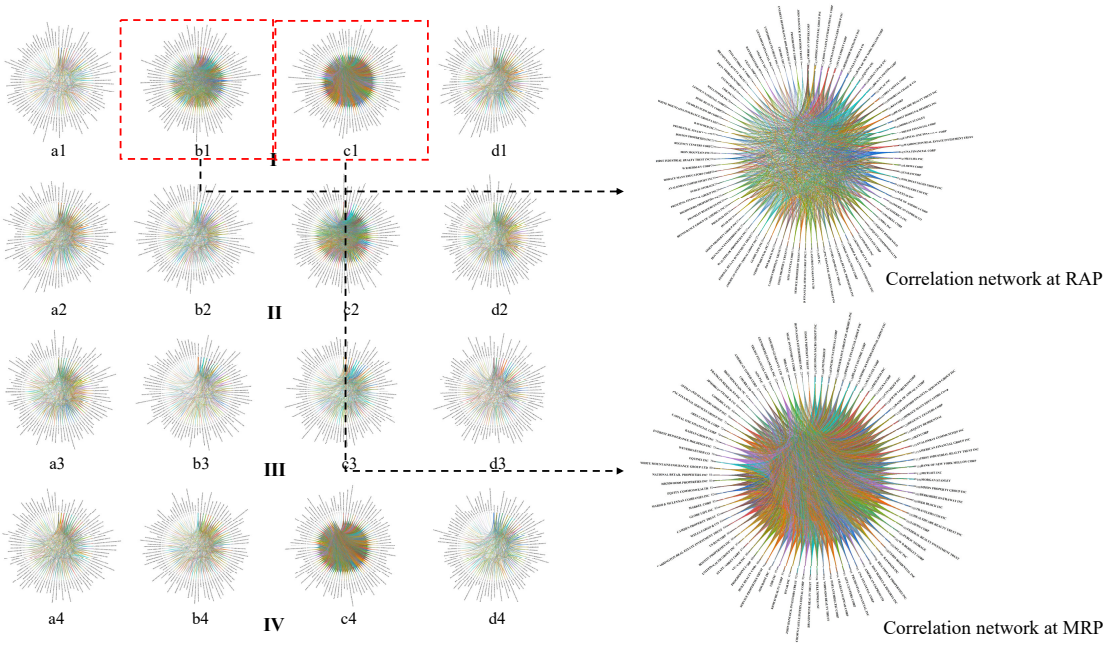

Figure 3: Granger causality network

surge stages. The accumulation stage of the 2015 shock (a3-b3) is longer than that of the 2010 (a2-b2) and 2020 (a4-b4) shocks, but the 2015 shock has the shortest surge stage (b3-c3). When the speed reaches its maximum and then rapidly turns negative, the 2015 shock exhibits the lowest risk peak during the 4 shocks.

Corresponding to the time division of four shock events above, we construct the Granger casuality network corresponding to each time point, we find that the changes of networks at 4 time point exhibit a consistent law in the four shocks. The densities of the correlation lines at SP and EP are similar. Compared to them, the strong correlation lines significantly increase between the RAP and the MRP, and the lines gradually become dense. Figure 4 shows the line of matrix between institutions at each point, where represents the correlation newtowk of the U.S. sample at SP (ai); RAP (bi); MRP (ci) and the point before the next shock EP (di) respectively. By comparison, we find the following. First, the correlation matrix in Figure 4-ai is relatively sparse and has not formed strong correlations; the correlation matrix in Figure 4-b is slightly enhanced; and the correlation matrix in Figure 4-c exhibits a generally strong correlation, which aligns with the findings of (Billio et al., 2012). Second, the strong correlation is a temporary phenomenon, which is consistent with the conclusions of (Brunnermeier and Pedersen, 2008; Niţoi and Pochea, 2019). As shown by Figure 4-d, the correlation decreases before the next shock occurs.

The correlation figure within the system at the MRP is denser than that of SP and EP. The correlation increases significantly during the shocks, which is consistent with the findings of (Billio et al., 2012; BEKAERT et al., 2014). The strong correlation is primarily formed in the risk surge stages of 2008, 2010, and 2020, so the network is concentrated at the MRP (Figure 4-c2, c2, c4). The correlation of the RAP in the 2015 shock is weaker than that of other shocks (Figure 4-c3).

We then simulate the FIA at RAP and MRP to observe the isolation effect. As the nodes are removed from the network, the liquidity spiral formed by shocks can be suppressed gradually. The simulation of the FIA exhibits a better effect at RAP, as we simulate isolation at the risk aggregation point and the maximum risk value point and observe the spiral weakening effect. The start and end points do not show the strong temporary correlations above and in the spiral surge in figure4. Figure 5 illustrates the policy effects of implementing FIA at the RAP and MRP points for each of the four shock events. The black line represents the R2 values obtained by implementing the FIA at the MRP (ci). The red line indicates the R2 curve obtained by implementing the FIA at the point of the RAP (bi) . The liquidity spiral decreases significantly after the FIA is implemented, and the FIA helps reduce the further spread of the liquidity spiral. This phenomenon is shown in Figure 5, The y-axis represents the percentage of simulated liquidity spiral in the network after removing nodes to the real market. The x-axis represents the number of removed nodes. The result shows that policy interventions and risk insulation in the early stages of a crisis are found to be superior across the board to rescue after systemic risk has fully exploded. If the system has not formed a general correlation (in the risk accumulation stage), selecting institutions that initially form a strong correlation to implement the FIA can effectively inhibit the development of the liquidity spiral. The simulation results of the dotted red line are significantly lower than those of the dotted blue line over the entire interval. Compared with (bi-ci) targeting the same institutions, the effect of FIA is more obvious in the risk accumulation stage ($a_i - b_i$). The FIA cannot stop the liquidity spiral but can effectively suppress the size and the peak of the spiral aggregation.

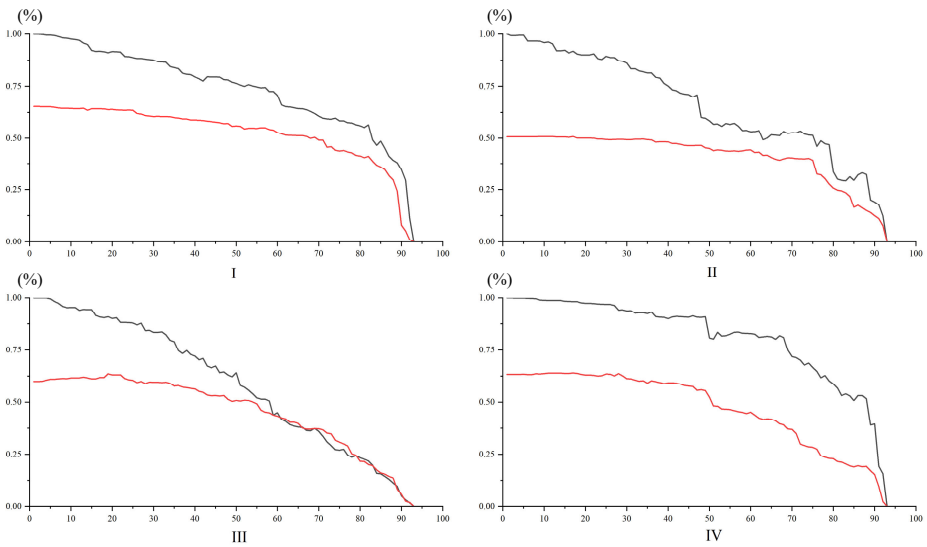

Figure 4: The effect of FIA

The liquidity spiral in the network shows a decreasing trend as the number of removing nodes increases, and the magnitude of the downward movement increases as more institutions entered into FIA. In figure 5-a, b and d, which demonstrate the shock events in 2008, 2010, and 2020, remove nodes from the network in the early stages of a crisis can

significantly inhibit the formation of strong correlations within the system, and at the same cost is generally more effective than intervening in a crisis after the risk has fully exploded. Figure 4-c illustrates the simulation result in 2015, the two curves converge after the number of removed nodes reaches 60, which is due to the fact that the financial shock in 2015 didn't form a serious impact on the U.S. market, and there was no general strong correlation within the market. Thus, after several number of institutions removing from the system, the remaining institutions in the network no longer generate risk spillover. The effects of FIA at the two points in time therefore show overlapping decreasing results.

If the system has not formed a general correlation (in the risk accumulation point), selecting institutions that initially form a strong correlation to implement the FIA can effectively inhibit the development of the liquidity spiral. The simulation results of the red line are significantly lower than those of the black line over the entire interval. Compared with (bi-ci) targeting the same institutions, the effect of FIA is more obvious in the risk accumulation stage (ai-bi). The FIA cannot stop the liquidity spiral but can effectively suppress the size and the peak of the spiral aggregation.

Implement FIA at RAP can effectively inhibit the formation of liquidity spirals in the network, which can achieve up to 40% in 2008, 2015 and 2020shock and increases with the number of isolated institutions, and is more significant in 2010 shock, where the reduction effect can achieve more than 50%. However, we should also note that although choosing the right timing for FIA can effectively suppress the liquidity spiral. But the marginal utility from increasing the number of removed nodes is not significant. As can be seen from the figure the slope of the descending curve remains almost horizontal in the first half. Of course, once the number of institutions exceeds half or more of the sample size, the effect will be more significant. In the most extreme case, choosing all institutions inevitably completely eliminates the liquidity spiral. This is equivalent to suspending the operations of all systems for risk control, which is obviously meaningless. It also suggests that only choose optimal timing will not complete the FIA' s fully policy design, and we must build on this with further discussion about how to block the wake-up call of liquidity spiral.

4.4 Optimal number of FIA

As we discussed above, after determining the isolation method and identifying the optimal isolation time point, we should to decide a defined number of nodes that been removed from the network. As can be seen from the results of the simulation charts, when the number of institutions that enter the FIA increases, the level of the liquidity spiral in the market decreases exponentially. The sharp decline of the liquidity spiral is concentrated after removing more than 60% institutions in the network. But it's unrealistic in the actual endogenous rescue problem because we have to consider the cost of implementing the rescue instrument; as the number of institutions with isolation buffers increases, it means that the cost of implementing the FIA increases. Simply increasing the number of institutions entering the FIA is a double-edged sword: on the one hand, as the number increases, the liquidity spiral decreases to an insignificant degree; on the other hand, an increase in the

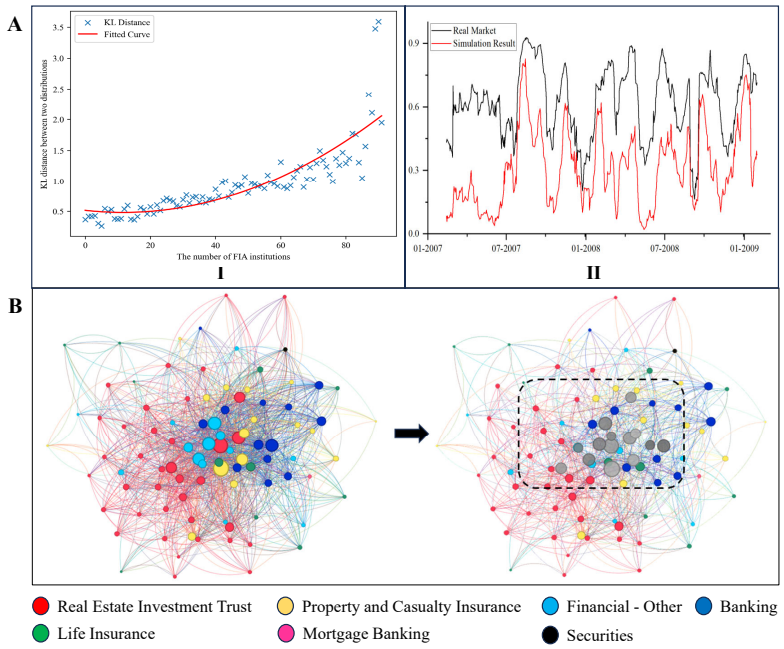

Figure 5: Simulation results in US GFC

number implies high cumulative costs, and great policies must minimize costs for optimal bailout results. There is a trade-off between a decreasing degree of liquidity spiral and increasing cumulative costs, with the goal of finding the most efficient rescue policy. In this way, we design an optimization model to find the optimal number of institutions which is the fuel should be removed to extinguish the fire of wake-up call.

By adding the percentage of cumulative market value as the penalty function, we solve the optimization model in Eq (15). Take the GFC in 2008 as an example, figure 6 A-I shows the fitted curve of objective function, and we can get the optimal number of FIA is 12. That means during the global financial crisis in 2008, when we detected the risk signal as a wake-up call, we can reduce the overall liquidity spiral degree to 60% by isolating 13% (12/93) of the key nodes in the network.

In order to achieve optimal result within a limited cost, we calculated the distribution of nodes' degree in the network. As shown in table 2-Panel A, The degrees of nodes in the network show a significant left-skewed distribution, indicating that the connected network among U.S. financial institutions is characterised by a distinctly small-world nature. Nodes located at the core of the network form extensive risk linkages with other nodes at the edge of the network. Figure 6 illustrates the comparison of inter-connected networks before and after FIA with the optimal number of FIAs during 2008 in the US, the size of a node in the figure represents its connected degree which calculated by Eq (11). from the left panel of figure 6 we can observe that at the RAP, the correlation network exhibits a significant "central-peripheral" structure. A few nodes at the canter of the network have more edges with each other, and most of the nodes lay on the margin of the network. On the contrary, in the right panel, when we remove some nodes at the optimal number.

The dense correlation aggregation in the network disappears and the degree of correlation between nodes shows a more uniform distribution. As we discussed above, the surge in intra-network correlations creates consistent behaviour between institutions and drives up the overall level of systemic risk. We argue that the centralised nodes in the network play a key risk contagion and driver role in the four stages of liquidity spiral formation. The stronger influencing they cause on other nodes in the network makes them an important factor in the creation, superimposition and amplification of liquidity risk. When we remove some important nodes in the network with the maximum degree strategy, the original correlation aggregation phenomenon will be weakened, and the degree distribution of the nodes will be close to the uniform distribution. At this point, the original liquidity risk contagion process loses its momentum and spillover path, and we block the liquidity spiral by 'removing the fuel to extinguish a fire', so that the entire network remains relatively healthy and stable in the face of external shocks.

By fusion trading in the network for some institutions at RAP, figure 6 A-II compares the real liquidity spiral trend and the results under scenario simulation. The simulation results of the liquidity spiral are significantly weakened. As shown by the red line in the figure, the simulated liquidity spiral still fluctuates over time and in response to the external shocks, but both the level and the duration of peaks are lower than it in the real market, which proves the effectiveness of the FIA.

Based on the method above, we observe that this optimal number exists but varies under different shocks. By solving Eq 11 using enumeration, we obtain the optimal number for the FIA.

Table 2: Node Degree Distribution and The Effect of FIA In US Market

Panel A: the node degree distribution in 4 shocks						
	Mean	Std	Min	Max	Skew	Kurt
2008	32	16.624	7	85	3.762***	1.543
2010	16	12.013	0	69	5.486***	3.952***
2015	11	8.115	0	41	3.824***	1.894*
2020	12	7.395	1	31	3.132***	-0.119
Panel B: the effect of FIA						
	shock event / R^2	Liquidity Injection / R^2	PC	optimal number	Original average R^2 /Simulation R^2	PC
2008	Jun-07	Feb-08		12	0.723	
	0.708	0.529	25.29%		0.465	35.75%
2010	Jul-11	Sep-12		8	0.613	
	0.698	0.416	40.30%		0.311	49.26%
2015	Aug-14	Sep-15		9	0.309	
	0.513	0.424	17.20%		0.189	38.75%
2020	Jan-20	Nov-20		18	0.588	
	0.791	0.382	51.80%		0.375	36.21%

Nodes: Panel A shows the degree distribution of nodes in the four shocks, *, **, *** denoting significant at the 10%, 5%, and 1% significant levels, respectively. Panel B reports the timing of the shock event and liquidity injection in turn, as well as the optimal number of FIA. PC denotes the percentage change in the liquidity spiral.

Table 2 shows the effect using R2. In Table 2, the Time event in the first column presents information about all four shocks. The original average R2 in the second column is from Eq. (7), which measure the liquidity spiral without FIA. The third (Time) and fourth (R2) columns under shock indicate the time and the liquidity commonality after the shock event. The fifth (Time) and sixth (R2/ PC) columns (under injection) indicate the time and the liquidity commonality and PC after the centralized liquidity injection event. Column seven indicates the optimal number of institutions participating in the FIA simulation, and columns eight indicate the liquidity commonality R2 from Eq. (8) and PC after implementing FIA at the optimal timing point (RAP) The original average R2 in the second column reveals that the liquidity commonality formed by the 2008 shock is the strongest, followed by that formed by the 2010 and 2020 shocks, while the least intense liquidity commonality is that formed by the 2015 shock. After the centralized liquidity injection event (column three) in 2022, the R2 drops by up to 51.80% (from 0.791 to 0.382). In the 2010 shock, the concentrated liquidity injection effect is 40.3%. In the 2015 shock, the liquidity injection effect is the weakest at 17.20%. The extents to which concentrated liquidity injection inhibits liquidity spirals significantly differ; ultimately, the lower-scale shock responds less to liquidity injection.

In the 2008 shock simulation, we find that having 12 institutions participate in the FIA

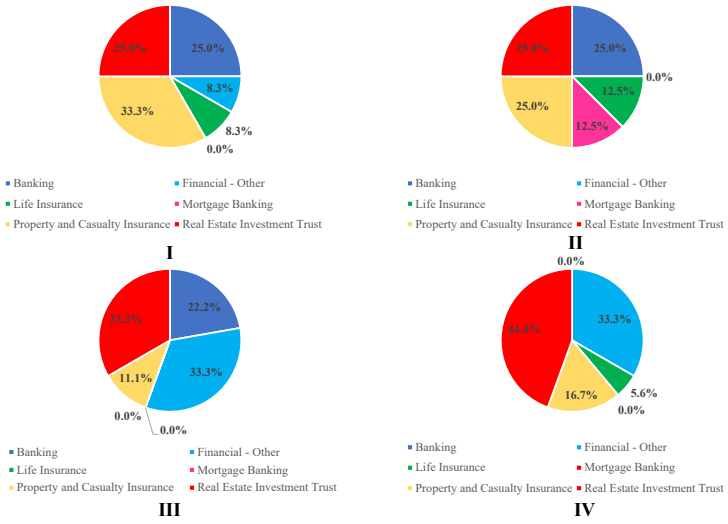

Figure 6: Proportion of FIA institutions' sectors

can reduce the original R2 value by 35.75%, as shown in table 2. Among these simulations, the effect of FIA has the most impact in the 2010 shock experiment. As we only control 9% (8/93) of institutions, and can reduce the total degree of liquidity spiral nearly 50%. In the 2015 and 2020 crises, we calculate the optimal number to be 9 and 18 based on the constrained optimisation model, respectively. The simulation results for four different periods yield consistent conclusions pointing to the fact that by using FIAs at the optimal time and in the optimal quantity, we can reduce the degree of liquidity spirals within the market by 35%-50% while controlling for the minimum cost (less than 20% of institutions). Notably, with the exception of the 2020 liquidity injection due to COVID-19, the FIA works better than the liquidity injection in all three simulations. On the one hand, liquidity injections can only dampen the spread of liquidity spirals in the short term, but they do not address the root causes of liquidity risk, so that correlation R^2, although it declines after a liquidity injection event, gradually rises to its average level again over time. In contrast to liquidity injections, the FIA's approach stops the deterioration of liquidity conditions within the market at its source, reducing the propagation of liquidity risk among the remaining institutions in the network by leave a serious of institutions out. 2020 shock was not due to systemic risk triggered by the financial crisis, so the timely liquidity injections led to a 51.8% drop in the degree of intra-market correlation. However, the simulation result by FIA also achieved a great decrease of 36.2%.

Figure 6 shows the percentage of sectors in which the isolated institutions belongs in the four simulations. In four cross-market shock events, the types and percentages of sectors that exhibit strong correlation within the system are different. The Real Estate (25%) and the Banking (25%) bore the brunt of the 2008 GFC, which in turn spread to other sectors such as Property and Casualty Insurance (33.3%), reflecting the impact of the subprime crisis on the financial system as a whole; Compared to 2008, the share of the Banking and Real Estate in the 2011 European debt crisis did not change, but the share of Mortgage banking

and Life insurance increased, and the distribution become more balance, reflecting a shift in the focus of the crisis to the broader financial sector, especially financial institutions and products related to the European debt problem; The impact of the 2015 stock market crash originated primarily in overseas markets, with a significant increase in the share of Financial-Others(33.3%). The overall industry distribution is more concentrated on financial institutions characterized by cross-market business linkages. In Figure 7-IV, The Real Estate (44.4%) and Financial-Others (33.3%) dominate the COVID-19 shocks, showing the impact of the epidemic on the real estate market and its vulnerability to global public health events. The increase in the proportion of financial-others in 2015 and 2020 also suggests that, as financial markets become more complex and dependent on financial instruments, financial institutions become more connected in the network, and risk linkages may involve a wider range of financial products and institutions. The dynamics of the number and type of sectors that accounted for the meltdown trades in the four shocks reaffirms that the FIA can adapt to different environments and market statuses to adjust the optimal risk truncation program implementation.

4.5 'Too big to fail' or 'Too interconnected to fail'?

In the above analysis, we explore the optimal time point and optimal number of FIA. Furthermore, we discuss the effectiveness and cost-saving advantages of the FIA. There is minimal difference between the PC in large institutions and high correlated small institutions; therefore, isolating small institutions is more cost-effective. We operate FIA simulations of a certain number of large institutions and the same number of strongly correlated small institutions, and the magnitude of the liquidity spiral is reduced in both simulations. Two subgroups are chosen from the sample: large institutions (L group) and correlated small institutions (S group). We select institutions with market values of more than $100 billion as the L group. The institutions with market values below $10 billion with a strong correlation (see Table B 2) are chosen as the S groups. Correspondingly, we select the same number of strongly correlated institutions in the S group for each shock interval. As shown in formula (2), the institutional trading volume VO and capacity MV are included to distinguish between the FIA effects on the L and S groups.

Figure 8 compares the effect of FIA between S and L group. The blue bar represents big group's percentage liquidity commodity compared with original market, and the red one indicate the S group. It can be seen that the application of FIA to small, highly connected institutions can have a very similar effect as controlling large companies. Firstly, when the transactions of large institutions or an equivalent number of strongly correlated small institutions are isolated, the magnitude of the liquidity spiral decreases, as both two bars remain at the level of 50%-70%. Second, there was little difference in the FIA between the L group and the S group. There is only little difference (nearly 5%) between the blue and red bars, and in 2015 simulation they are almost overlap. In the simulations, applying the FIA to small institutions with strong correlations is as effective as applying it to the same number of large institutions. That is, suspending the transactions of large institutions and

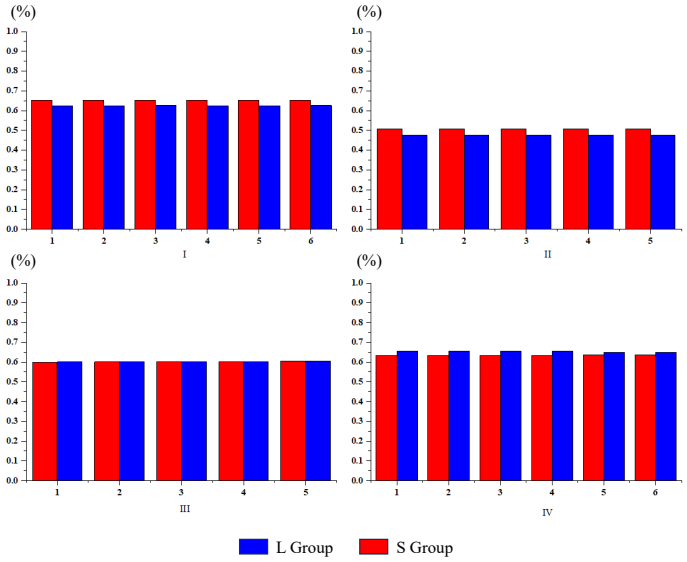

Figure 7: FIA in L and S group

the formation of initial strong correlations among small institutions suppress the negative effects caused by large-scale fire sales in the market. Both strategies can control the development of the liquidity spiral. Suspending the trading volume of large institutions in the market considerably reduces the amount of fire sales. A reduction in overall liquidity demand stabilizes prices, limiting the potential for further fire sales and asset depreciation.

Table 3 shows more detail between the results of the L group and S group. The maximum difference between the PC of the two groups is only 3.8%. This difference is from the 2015 shock simulation, in which the L group PC is 30.41% and the S group pc is 26.58%. The 2010 shock and the 2020 shock exhibit cases where the PC from the S group is better. In the 2010 shock, with five FIA institutions in each group, the PC of the L group is 45.91%, and that of the S group is 46.74%. In the 2020 shock, with six FIA institutions in each group, the PC of the L group is 40.89%, and that of the S group is 43.65%.

Table 3: FIA between L and S group

Time	Items Frozen	Original average R^2	Large /Percent change	Small /Percent change
2008	6	0.621	0.385	0.395
			38.09%	36.48%
2010	5	0.520	0.281	0.277
			45.91%	46.74%
2015	5	0.287	0.199	0.21
			30.41%	26.58%
2020	6	0.417	0.247	0.235
			40.89%	43.65%

Notes: Items Frozen is the number of nodes removed from the network. Column Large means removing institutions sorted by market value. Small denotes selecting the same number of institutions with large group by connection degree in the small group.

Although the individual trading volume of the S group is limited, this simulation selects small institutions that initially form a strong correlation and suspends multiple small institution transactions exhibiting the same behaviours (fire sales) at the same time. The FIA reduces the scale effect of their fire sale in shocks. A sufficient reduction in the number of fire sales can reduce overall liquidity demand and stabilize prices. As a result, it also slows the development of further co-movement, enabling it to further inhibit the liquidity spiral.

From a cost perspective, suspending large institutional transactions clearly requires greater expenditure. For regulators, choosing the appropriate time to restrict the transactions of small institutions with correlations can more economically suppress the amplifying effect of liquidity spirals during shocks.

5 Robustness check

In the same steps as this paper's empirical analysis using U.S. data, we show the empirical results of the FIA conducted in the European market in SUPPLEMENTARY MATERIALS.

6 Conclusion

Frequent and continuous reliance on injecting liquidity into systemically important institutions to mitigate crises has brought increasing disadvantages to the financial system, such as the abnormal rise in inflation rates, the transfer of a large amount of risk from individual financial institutions to the government and moral hazard. These disadvantages cannot be ignored. Following the other research approach, self-rescue, we proposed a series of reference standards forming the freeze isolation approach (FIA) from three aspects: how regulators participate, when participation occurs, and how many institutions

participate. We also conducted empirical testing on this approach.

First, the design of FIA through correlation network isolation can control the spread of risks and address insufficient liquidity in the system during shocks. We established the correlation based on the Granger causality matrix to identify institutions that contribute significantly to risk spread, avoiding the inefficiency of indirect crisis rescue methods that can only be approached by important institutions. By simulating and isolating transactions with some highly correlated institutions, wake-up calls of liquidity spirals can be blocked and the contagion of crises can be further reduced. Based on the dynamic Granger causality adjusted by Gray correlation, the FIA identifies the institutions that initially show strong correlations before a widespread co-movement is formed. Isolating the initial institutions from the market can slow the development of liquidity spirals.

Second, isolation simulations have better rescue effects at the maximum speed than at other points. We identified different spiral change points and constructed the correlation matrix for different time points. We conducted the FIA at different time points and observed that a considerable cost is associated with suppressing the development of a liquidity spiral in an already strongly correlated system. Moreover, conducting the FIA during the interval of the maximum speed is more effective than conducting it at other intervals, such as the point of the highest risk value.

Third, the FIA includes a constrained optimization model for determining the optimal number of participating institutions for different shock intervals. We used this quantity to isolate large or small institutions separately. The effect of isolating small institutions with initially high correlation is minimally different from that of isolating large institutions. This is good news for regulators, as fewer institutions at the border of marginal effects can be selected for the FIA. Our findings may provide valuable information for regulators to improve the efficiency of risk controls.

The FIA is designed from an isolation-related perspective to overcome the problems caused by external liquidity injection. It can also overcome the problems of insufficient rescue funds, delayed rescue opportunities, and insufficient participation in the original self-rescue plan due to the lack of regulatory perspective, which result in insignificant rescue effects. In the future, more detailed research on the operation of isolation institutions will be explored.

References

Acharya, Viral, Lasse H Pedersen, T. Philippon, and M. Richardson, 2017, Measuring systemic risk, *Review of Financial Studies* 30, 2–47.

Adrian, T., and M. K. Brunnermeier, 2016, Covar, *American Economic Review* 106, 1705–1741.

Ahnert, Toni, and Christoph Bertsch, 2022, A wake-up-call theory of contagion, *Review of Finance* 26, 829–854.

Antzoulatos, Angelos A., Kostas Koufopoulos, Costas Lambrinoudakis, and Emmanuel Tsiritakis, 2016, Supply of capital and capital structure: The role of financial development, *Journal of Corporate Finance* 38, 166–195.

BEKAERT, GEERT, MICHAEL EHRMANN, MARCEL FRATZSCHER, and ARNAUD MEHL, 2014, The global crisis and equity market contagion, *Journal of Finance* 69, 2597–2649.

Billio, Monica, Roberto Casarin, Michele Costola, and Andrea Pasqualini, 2016, An entropy-based early warning indicator for systemic risk, *Journal of International Financial Markets, Institutions and Money* 45, 42–59.

Billio, Monica, Mila Getmansky, Andrew W. Lo, and Loriana Pelizzon, 2012, Econometric measures of connectedness and systemic risk in the finance and insurance sectors, *Journal of Financial Economics* 104, 535–559.

Brunnermeier, Markus K, and L. H. Pedersen, 2008, Market liquidity and funding liquidity, *Review of Financial Studies* .

Chabot, Miia, and Jean-Louis Bertrand, 2021, Complexity, interconnectedness and stability: New perspectives applied to the european banking system, *Journal of Business Research* 129, 784–800.

Chen, Nan, Xin Liu, and David D. Yao, 2016, An optimization view of financial systemic risk modeling: Network effect and market liquidity effect, *Operations Research* 64, 1089–1108.

Chordia, Tarun, Richard Roll, and Avanidhar Subrahmanyam, 2001, Market liquidity and trading activity, *The Journal of Finance* 56, 501–530.

Cincinelli, Peter, Elisabetta Pellini, and Giovanni Urga, 2022, Systemic risk in the chinese financial system: A panel granger causality analysis, *International Review of Financial Analysis* 82, 102179.

Ebrahimi, Nader, Esfandiar Maasoumi, and Ehsan S. Soofi, 1999, Ordering univariate distributions by entropy and variance, *Journal of Econometrics* 90, 317–336.

Elliott, Matthew, Benjamin Golub, and Matthew O. Jackson, 2014, Financial networks and contagion, *American Economic Review* 104, 3115–53.

Gandy, Axel, and Luitgard A. M. Veraart, 2016, A bayesian methodology for systemic risk assessment in financial networks, *Management Science* 63, 4428–4446.

Gofman, Michael, 2017, Efficiency and stability of a financial architecture with too-interconnected-to-fail institutions, *Journal of Financial Economics* 124, 113–146.

Hameed, Allaudeen, Wenjin Kang, and S. Viswanathan, 2010, Stock market declines and liquidity, *The Journal of Finance* 65, 257–293.

Heider, Florian, Marie Hoerova, and Cornelia Holthausen, 2015, Liquidity hoarding and interbank market rates: The role of counterparty risk, *Journal of Financial Economics* 118, 336–354.

Jackson, Matthew O., and Agathe Pernoud, 2024, Credit freezes, equilibrium multiplicity, and optimal bailouts in financial networks, *Review of Financial Studies* 37, 2017–2062.

Jiang, Lei, Ke Wu, and Guofu Zhou, 2018, Asymmetry in stock comovements an entropy approach, *Journal of Financial and Quantitative Analysis* 53, 1479–1507.

Karaca, Yeliz, and Majaz Moonis, 2022, *Chapter 14 - Shannon entropy-based complexity quantification of nonlinear stochastic process: diagnostic and predictive spatiotemporal uncertainty of multiple sclerosis subgroups*, 231–245 (Academic Press).

Karolyi, G. Andrew, Kuan-Hui Lee, and Mathijs A. van Dijk, 2012, Understanding commonality in liquidity around the world, *Journal of Financial Economics* 105, 82–112.

Moshirian, Fariborz, Xiaolin Qian, Claudia Koon Ghee Wee, and Bohui Zhang, 2017, The determinants and pricing of liquidity commonality around the world, *Journal of Financial Markets* 33, 22–41.

Niţoi, Mihai, and Maria Miruna Pochea, 2019, What drives european union stock market co-movements?, *Journal of International Money and Finance* 97, 57–69.

Pacelli, Vincenzo, Federica Miglietta, and Matteo Foglia, 2022, The extreme risk connectedness of the new financial system: European evidence, *International Review of Financial Analysis* 84, 102408.

Paltalidis, Nikos, Dimitrios Gounopoulos, Renatas Kizys, and Yiannis Koutelidakis, 2015, Transmission channels of systemic risk and contagion in the european financial network, *Journal of Banking Finance* 61, S36–S52.

Wang, Gang-Jin, Zhi-Qiang Jiang, Min Lin, Chi Xie, and H. Eugene Stanley, 2018, Interconnectedness and systemic risk of china's financial institutions, *Emerging Markets Review* 35, 1–18.

Wang, Gang-Jin, Chi Xie, Kaijian He, and H. Eugene Stanley, 2017, Extreme risk spillover network: application to financial institutions, *Quantitative Finance* 17, 1417–1433.

Wang, Gang-Jin, Shuyue Yi, Chi Xie, and H. Eugene Stanley, 2021, Multilayer information spillover networks: measuring interconnectedness of financial institutions, *Quantitative Finance* 21, 1163–1185.

Wu, Guangdong, Zhibin Hu, Huanming Wang, and Bingsheng Liu, 2024, Adding sectors or strengthening ties? adaptive strategies for cross-sector collaboration in disaster governance, *Public Management Review* 1–23.

Appendix A: Calculation of Delta CoVaR and MES

Delta CoVaR is defined as at a certain holding period and a given level of confidence (1-q)% ; when an institution is in an extreme loss situation, the value at-risk of the whole system (Adrian and Brunnermeier, 2016). The main idea is to quantify the systematic risk spillover effect of institutions on the market through the tail joint probability distribution.

In this paper, we calculate the Delta CoVaR by quantile regression: X_t^i is the log-return of institution i at time t, $X_t^{system|i}$ is the log-return of the whole system at time t and M_{t-1} is the macro-state variable.

$$X_t^i = \alpha_q^i + \gamma_q^i M_{t-1} + \varepsilon_{q,t}^i \tag{A.1}$$

$$X_t^{system|i} = \alpha_q^{system|i} + \gamma_q^{system|i} M_{t-1} + \beta_q^{system|i} X_t^i + \varepsilon_{q,t}^{system|i} \tag{A.2}$$

We use quantile regression to estimate the parameters of the above equation. By solving the objective function, we achieve the adjustment of the parameter coefficients and approximate the estimated value to the true value:

$$\underset{\alpha_q,\beta_q,\gamma_q}{min} \sum\nolimits_t \left\{ \begin{array}{c} q\% \left| X_{t+1}^j - M_t\beta_q - R_{t+1}^i\gamma_q \right| \text{if} X_{t+1}^j - M_t\beta_q - R_{t+1}^i\gamma_q \geq 0 \\ (1-q\%) \left| X_{t+1}^j - M_t\beta_q - R_{t+1}^i\gamma_q \right| \text{if} X_{t+1}^j - M_t\beta_q - R_{t+1}^i\gamma_q < 0 \end{array} \right\} \tag{A.3}$$

Substituting the parameters into the following equation, we calculate Delta CoVaR as an indicator of the systemic risk spillover effect of institution i on the system: